SEMARAK ILMU PUBLISHING

Journal of Advanced Research in Fluid Mechanics and Thermal Sciences

Journal homepage:
https://semarakilmu.com.my/journals/index.php/fluid_mechanics_thermal_sciences/index
ISSN: 2289-7879

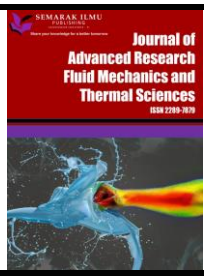

The Influence of Varying Ar/O_2 Gas Ratio with Catalyst-Free Growth by Homemade Thermal Evaporation Technique

Azira Khairudin[1], Najiha Hamid[1], Syahida Suhaimi[2,*], Mohd Ikmar Nizam Mohamad Isa[3], Nur Athirah Mohd Taib[1], Syamsul Kamar Muhamad @ Wahab[1]

[1] Faculty of Science and Technology, Universiti Sains Islam Malaysia, 71800 Nilai, Negeri Sembilan, Malaysia
[2] Nano Energy Lab (NEL), Energy Materials Consortium (EMC), Faculty of Science and Technology, Universiti Sains Islam Malaysia, 71800 Nilai, Negeri Sembilan, Malaysia
[3] Energy Materials Consortium (EMC), Advanced Materials Team, Ionic & Kinetic Materials Research (IKMaR) Laboratory, Faculty of Science and Technology, Universiti Sains Islam Malaysia, 71800 Nilai, Negeri Sembilan, Malaysia

ARTICLE INFO

Article history:
Received 1 February 2024
Received in revised form 28 May 2024
Accepted 9 June 2024
Available online 30 June 2024

Keywords:
Zinc oxide; thermal evaporation gas flow rate; purity

ABSTRACT

A nanostructured zinc oxide (ZnO) with different percentages of argon and oxygen gas flow rate was deposited on a silicon wafer by a simple hot tube thermal evaporation technique. The effect of different percentages of gas flow rate on the crystal structure, surface morphology and optical properties were characterized using X-ray diffraction (XRD), field emission scanning electron microscopy (FESEM), energy dispersive X-ray (EDX) and RAMAN spectroscopy, respectively. The changes of morphologies from FESEM were significant where the grown ZnO nanostructures show three different shapes which are nanotripods, nanoclusters and nanorods at 5%, 10% and 25% of oxygen gas, respectively. EDX results revealed that Zn and O elements have a major percentage in the sample indicating a composition has high purity of ZnO. XRD patterns displayed the most intense diffraction peak of ZnO at (101), which exhibited a single crystalline hexagonal structure with preferred growth orientation in the c-axis. RAMAN scattering study found that synthesized ZnO shows the high intensity of E2 mode and low intensity of E1 mode attributed to all the samples having good crystal quality containing fewer structural defects. In conclusion, the E15 sample with a 25% oxygen gas flow rate was selected as an optimum result for synthesizing a homogenous surface and high crystallinity of ZnO by using a hot tube thermal evaporation process. This work can enhance the development of ZnO production in various applications.

1. Introduction

Zinc Oxide (ZnO) is an important II-IV type semiconductor that has a direct band gap of 3.37 eV and a high exciton binding energy of 60 meV at room temperature [1-3]. ZnO has emerged as the preferred material for use in situations of great heat, high power, and short wavelength, making it excellent for electronic and optoelectronic devices [4]. Other favourable characteristics of ZnO is non-toxic, cheap and relatively abundant source of materials besides titanium dioxide and arsenide [5].

* *Corresponding author.*
E-mail address: syahida@usim.edu.my

https://doi.org/10.37934/arfmts.118.2.101113

ZnO also can be synthesized as a large single crystal by many types of techniques and is possible to be grown in various dimensions.

Many techniques have been used to synthesize ZnO nanostructures such as sol-gel, pulsed laser deposition, RF sputtering, hydrothermal process and spray pyrolysis [6-15]. However, the vacuum thermal evaporation technique was used in this work due to several advantages. Thermal evaporation technique with a low vacuum provides the mean free path of vapour atoms in laminar flow as the vacuum chamber dimension, so these evaporated particles can travel in a straight line from the source towards the substrate resulting in a large area deposition of ZnO nanostructures [16].

Besides, in this work, a simple hot tube thermal evaporation system was developed at low-cost and self-catalyzed growth that does not require the high vacuum apparatus favourable to be used in industry. Specifically, zinc metal as a source was loaded and placed at the centre of the quartz tube while Si wafer as substrate was inserted at the end of the quartz tube at the outlet side. Si wafer with (100) orientation was used as a substrate for growing ZnO in order to reduce lattice mismatching compared to bare Si wafer [17].

The effect of varying percentages of argon and oxygen gas flow rate towards the structural and optical properties was investigated in detail. Nanoscale morphologies, encompassing zero-dimensional (0D), one-dimensional (1D), and two-dimensional (2D) nanostructures, have been extensively researched for their fundamental scientific significance and practical applications in nanoelectronics, nanomechanics, and flat panel displays, with 1D ZnO nanostructures demonstrating unique properties due to quantum confinement effects and their exceptionally high surface-to-volume ratio [18,19]. In advancements of engineering, the remarkable ability of nanoparticles to pass through filters and penetrate surfaces makes them a promising lubricant additive, effectively reducing friction and ensuring long-term engine protection [20]. Hence, ZnO nanostructures have the potential to revolutionize electronic and optoelectronic devices. These structures have been shown to enhance the efficiency and performance of various optoelectronic devices, including LEDs, solar cells, and photodetectors. When integrated into electronic devices, ZnO nanostructures notably improve conductivity, durability, and environmental sustainability. This underscores the importance of ongoing research in this area, highlighting the promising future prospects of ZnO nanostructures in advancing electronic and optoelectronic technologies [18,21].

Huang *et al.,* [22] have reported the effect of Ar:O_2 gases flow ratio on the cathodic vacuum arc properties of ZnO deposition. Meanwhile, Rasheed *et al.,* [23] have worked on the effect of gas sputtering flow rate towards structural and electrical properties of ZnO/Cu/ZnO membrane. By using reactive DC pulsed magnetron sputtering, Camacho-Berrios *et al.,* [24] investigate the impact of elevating the partial pressure of oxygen in the sputtering gas, varying it from 20% to 70% O_2/Ar, on the properties of Zinc Oxide thin films. Abdulgafour *et al.,* [19] reported the customized structure, morphology, optical properties, and growth progression of ZnO nanostructures fabricated on quartz substrates utilizing the wet thermal evaporation technique by varying rates of Ar and wet O_2 gas flow. Even though a large number of studies were reported regarding synthesizing ZnO nanostructures by thermal evaporation yet still only a few have reported synthesis of ZnO nanostructures without any catalyst using Si substrate (100) varying percentages of gas flow rate.

2. Methodology

2.1 Synthesis of Zinc Oxide

ZnO nanostructures were synthesized by thermal evaporation method at 800℃ for 90 minutes at a vacuum pressure of 2.0 x 10^{-2} torr as shown in Figure 1. Firstly, Si wafer <100> with (1 x 1) cm

dimension as deposited substrate was cleaned with methanol and followed with a distilled water rinse several times. High purity of Zinc (99.99%) was chosen as source material and weighed at 1g before putting into an alumina boat. The source and substrate were loaded into the centre of a quartz tube that was (50 x 1000) mm in size, with a 15 cm gap between them. Next, the rotary pump was switched on for 5 minutes to remove undesirable gases or particles from the system to avoid any contamination. It was also possible to achieve temperature quickly as the pressure was reduced. Then, the furnace was set to the desired temperature at 800℃ and 95% of carrier gas (Ar) was introduced. At 800℃, the reactant gas which is O_2 gas with 5% was introduced in the vacuum chamber controlled by a flow meter. The reaction was completed at 90 minutes and both gases were stopped to let the furnace cool down at room temperature before the synthesized ZnO was taken out. The experiment was repeated with 10% and 25% of the O_2 gas flow rate.

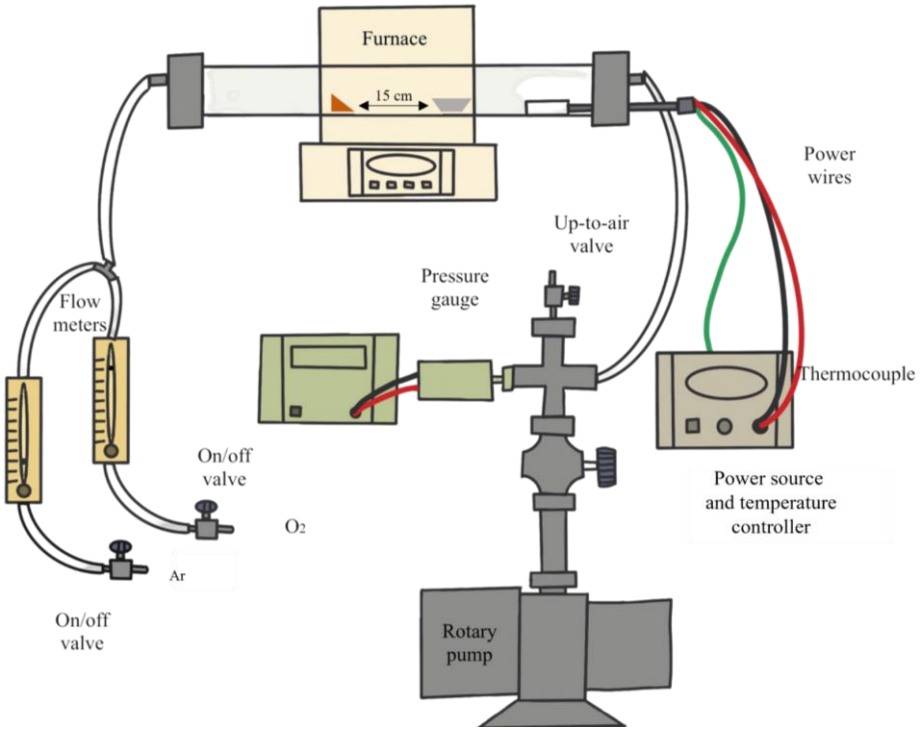

Fig. 1. Schematic diagram of Hot Tube Thermal Evaporation (HTTE) system

2.2 Characterization of Zinc Oxide

Grown ZnO nanostructures were characterized for structural and optical properties. The surface morphology of all samples was characterized using a field emission scanning electron microscope (FESEM, JOEL JSM-IT800) with X-ray energy dispersive spectroscopy (EDS). Meanwhile, Miniplex X-ray diffraction (XRD) with Cu Kλ radiation ($\lambda = 1.5406$ Å) was used to study the crystalline structure of synthesized ZnO. The XRD pattern was recorded in the 2θ range of 20°-80° at the scanning speed of 2° per minute and the crystallite site (D) of the samples was calculated by using Scherrer's equation:

$$D = \frac{K\lambda}{\beta cos\theta}$$

Horiba HR-800 confocal RAMAN microscope equipped with He-Cd laser at 532 nm line was used to investigate the optical properties of ZnO nanostructures.

3. Results and Discussion

3.1 FESEM Characterization

FESEM was used to obtain the morphology of the ZnO nanostructures. It can be seen that different morphologies were grown on the Si wafer with different O_2 gas flow rates. Varying O_2 gas flow rates could affect much on the structural properties of ZnO nanostructures, especially in their size and shape. Table 1 below shows the percentage ratio of O_2 and Ar gas flow.

Table 1
Percentage of gas flow rate

Name of sample	Oxygen gas (%)	Argon gas (%)
E13	5	95
E14	10	90
E15	25	75

Figure 2 clearly shows that the whole substrate surface was covered with high-density and randomly oriented ZnO nanostructures when the sample was grown at 25% O_2 gas and 75% Ar gas flow rate. The flow rate of gases has such impacts on the formation of the ZnO nanostructures in different shapes including a tetrapod as shown in Figure 2. The high density of the randomly oriented ZnO nanostructures is indicated by the fraction of nanostructures grown on the substrate to the empty spaces between them. The growth of high-density ZnO nanostructures on Si (100) bulk substrates was achieved at 25% of the O_2 flow rate [25]. Figure 2(a) revealed dense ZnO consists of nanoparticles and tripod-like structures with lengths ranging between 200-300 nm. Meanwhile, Figure 2(b) shows the synthesized ZnO nanostructures at 50 kX image with diameter was varied and their length was extended to several microns.

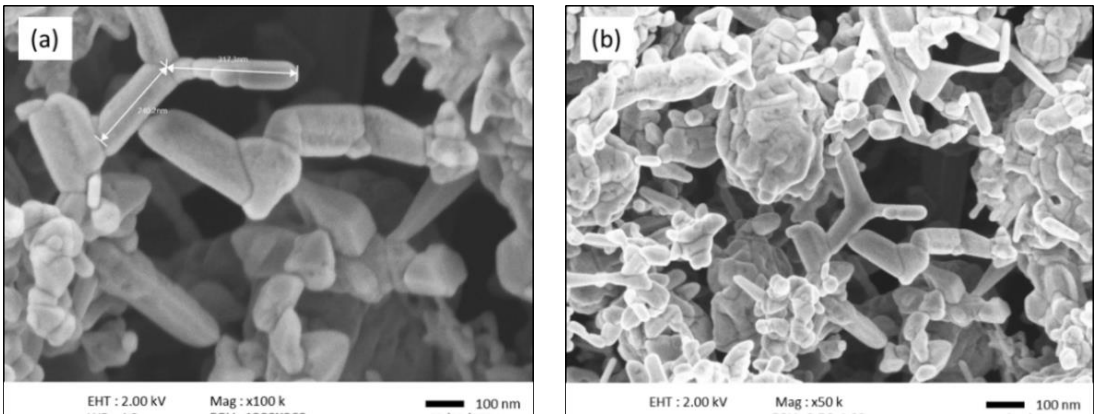

Fig. 2. ZnO nanostructures with 25% of O_2 gas flow rate (a) magnification at 100kX and (b) magnification at 50kX

As the flow rate was increased, the nanostructures changed to tetrapod nanowires with hexagonal cylinder legs. The legs have a length of around 200 nm to 300 nm and the tetrapods fully covered the substrate underneath it. It is worth noting that having a higher flow meter of the gases has helped in providing appropriate surfaces or planes for ZnO seed nucleation at the initial stage so the subsequent growth of ZnO nanowires can be promoted.

The FESEM image in Figure 3(a) shows the synthesized ZnO has morphology in the form of granular structure as the O_2 is decreased to 10%. The phenomena lead to the existence of particle agglomeration in the sample. Figure 3(b) reveals the FESEM image of ZnO has a uniform distribution of nanoclusters over the entire surface. The changes in shape can be explained based on the

introduction of O_2 gas as the amount is increased [12,26,27]. The flow meter of the gases plays an important parameter in controlling the morphology of the nanostructures.

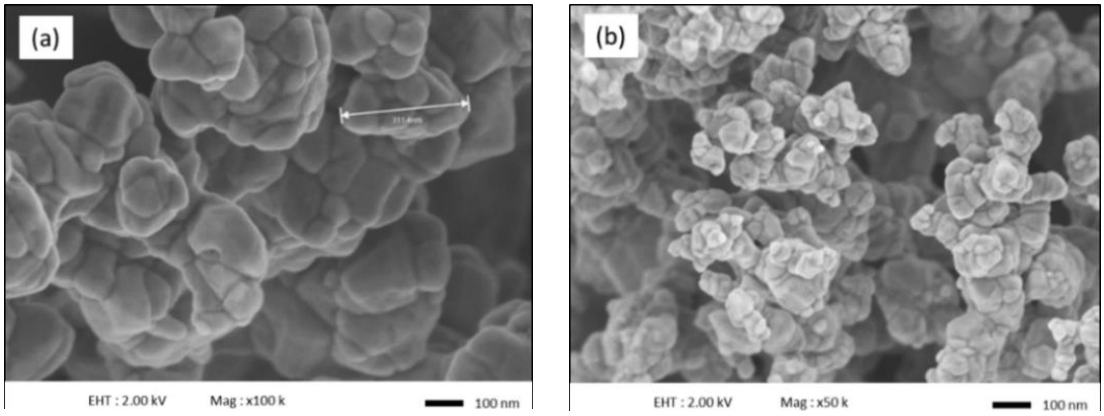

Fig. 3. ZnO nanostructures with 10% of O_2 gas flow rate (a) magnification at 100kX and (b) magnification at 50kX

As the O_2 gas flow rate was further reduced to 5% and the percentage value of the Ar gas flow rate was increased to 95%, the nanoparticles grew bigger and formed new nanoclusters with several nanorods as shown in Figure 4. Since ZnO heavier than Zn and O_2 causes the development of the base for new nanostructures to grow. Moreover, there is no catalyst was added to the experiment. Thus, it is very typical that a nanorod is formed at the tips of nanoclusters during the growth process and possesses a sharp tip [28-31]. This growth process follows the vapor solid (VS) mechanism. It could be observed that the surface morphology of synthesized ZnO was appreciably influenced by the percentage of O_2 and Ar gas flow rate that was introduced in the vacuum chamber. Thus, it was affirmed that varying gas flow rate plays a crucial part in controlling the nucleation and growth of ZnO nanostructures.

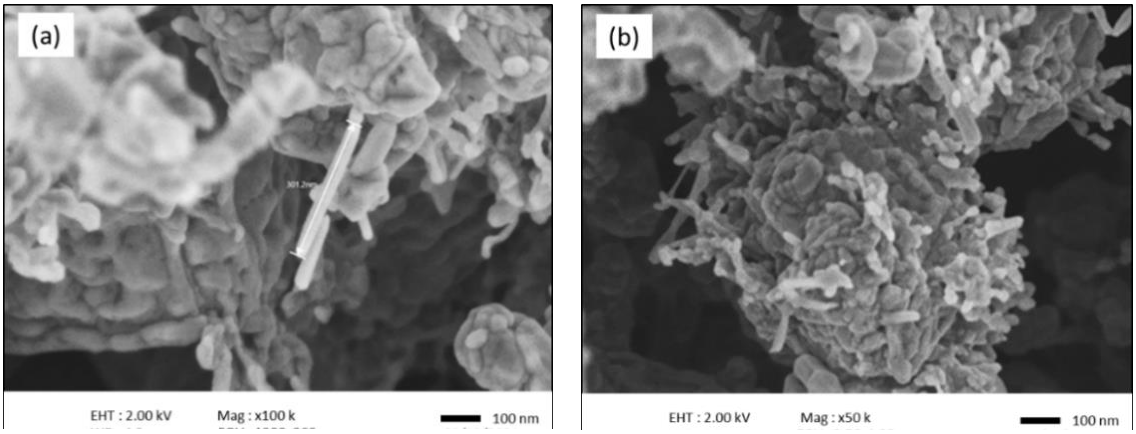

Fig. 4. ZnO nanostructures with 5% of O_2 gas flow rate (a) magnification at 110kX and (b) magnification at 75kX

As the flow rate of the gases increases, the nucleation of Zn particles increases thus resulting in increasing the formation of ZnO nanoclusters. Typically, the products consist of a majority of wire-like ZnO and nanoclusters that exhibit an agglomeration morphology that gradually transforms into wire-like and tetrapod nanostructures. From the FESEM images, it can be interpreted that at a flow meter of 25% O_2, very differently shaped structures were synthesized due to the increase of speed of

the gas molecules in the chamber that facilitate the diffusion mechanism of source atoms through the substrate [26].

3.2 EDX Spectra

Energy dispersive X-ray (EDX) is used to determine the purity and composition of the synthesized sample. Figure 5 depicts the EDX analysis recorded at three different percentages of O_2 gas flow rates which are 5%, 10% and 25%. As observed in the spectrums above, the C element probably is the result of a heating process while the Na and Al elements are likely from the material of the substrate holder. Nevertheless, the obtained ZnO sample is considered high quality because it was found that the Zn and O elements dominated the percentage of the materials when compared to other existing elements in the samples.

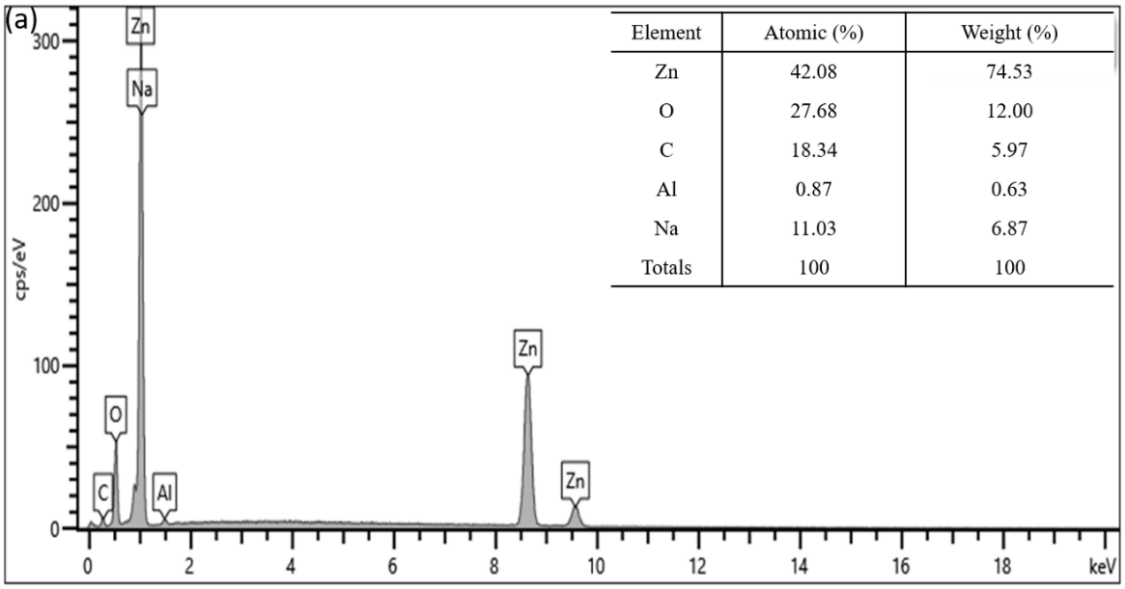

Element	Atomic (%)	Weight (%)
Zn	42.08	74.53
O	27.68	12.00
C	18.34	5.97
Al	0.87	0.63
Na	11.03	6.87
Totals	100	100

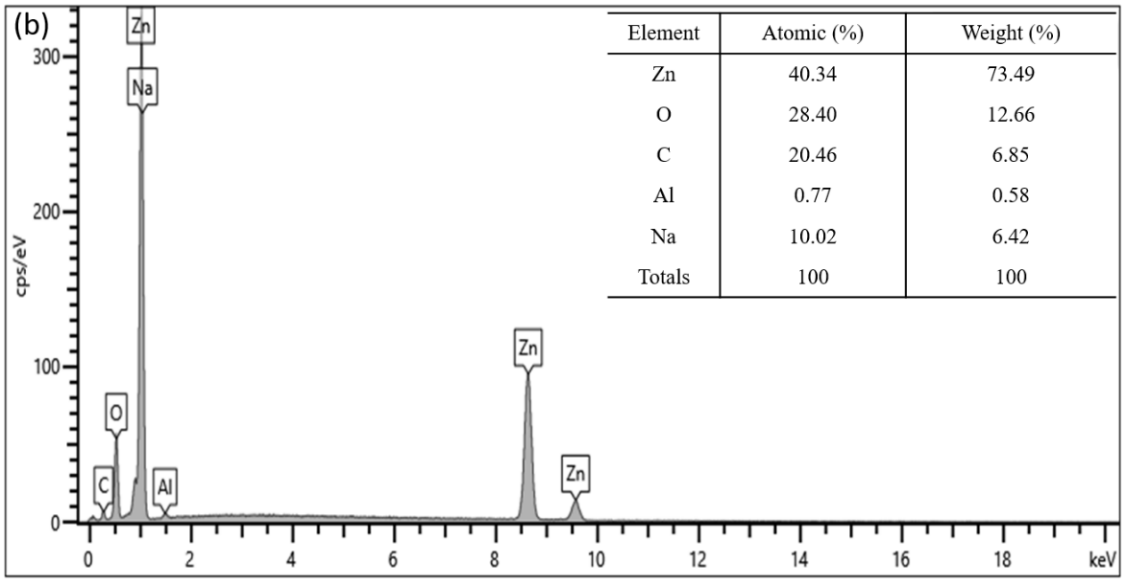

Element	Atomic (%)	Weight (%)
Zn	40.34	73.49
O	28.40	12.66
C	20.46	6.85
Al	0.77	0.58
Na	10.02	6.42
Totals	100	100

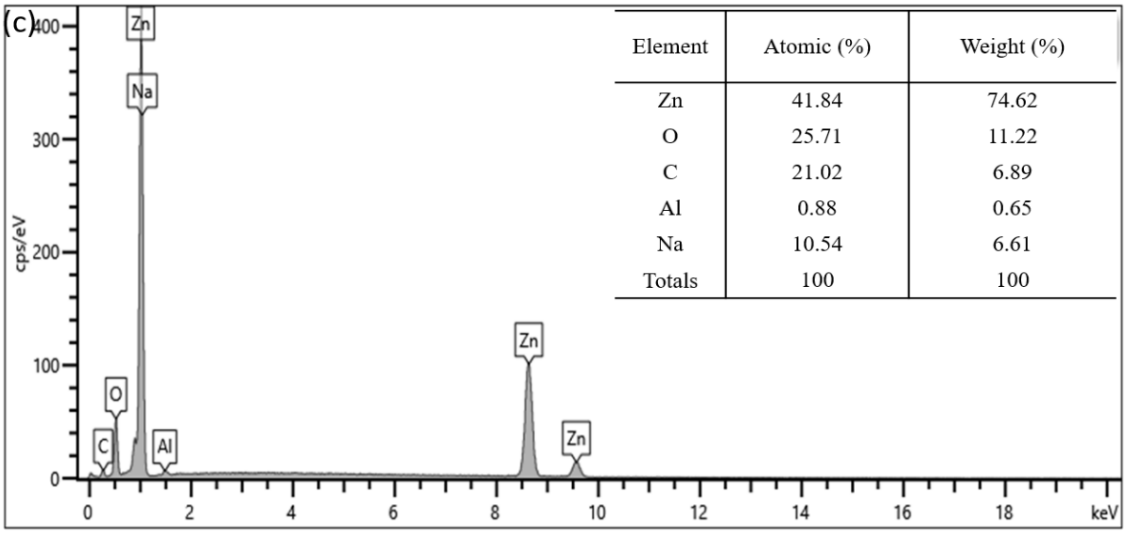

Element	Atomic (%)	Weight (%)
Zn	41.84	74.62
O	25.71	11.22
C	21.02	6.89
Al	0.88	0.65
Na	10.54	6.61
Totals	100	100

Fig. 5. EDX spectra with different O_2 gas flow rate (a) 25%, (b) 10%, and (c) 5%

3.3 XRD Characterization

Figure 6 displays the gas flow rate-dependent XRD spectra of pure synthesized ZnO which comprises a few sharp peaks attributed to the high purity phases of ZnO nanocrystalline. Samples E13, E14 and E15 were synthesized by varying percentages of O_2 gas flow rates which are 5%, 10% and 25%, respectively. All observed peaks have been indexed to hexagonal wurtzite structures with (101) orientation on the plane at angle $2\theta \approx 35.84°$, corresponding to COD ID card #1011259 in the absence of any impurity phases. It is observed that E13 (5% O_2) and E15 (25% O_2) have an intense diffraction peak at (101) indicating the synthesized ZnO were highly oriented, implying a c-axis growth perpendicular to the substrate surface. The results agreed with studies by Das *et al.,* [32] and Mugwang'a *et al.,* [33] which synthesized ZnO has a high crystalline structure and is well-established. Whereas, E14 (10% O_2) has a low peak of (100) indicating low crystallinity. Thus, the gas flow rate has a significant effect on the crystallinity of ZnO which involves the nucleation and growth mechanism.

The growth of catalyst-free ZnO nanostructures was governed by the Vapor-Solid (VS) mechanism. The surface energy of a plane is related to the effectiveness of capturing the adsorbed atoms and decides the growth rate and the proportion of crystallographic planes such as (001), (100) and (101) in the final structure under certain supersaturation levels of Zn and O vapors. In the case of ZnO grown with a different flow rate of gases ratio, the (101) planes have the lowest surface energy, followed by (102) planes.

The XRD data were further analyzed to evaluate the average crystallite size of synthesized ZnO. The crystallite size was calculated using the Scherrer equation $D = k\lambda/\beta cos\theta$ where k = 0.9 is the geometrical constant, λ = 0.1542 nm is the wavelength of the X-ray used, β is the FWHM in radian and θ is the reflection angle.

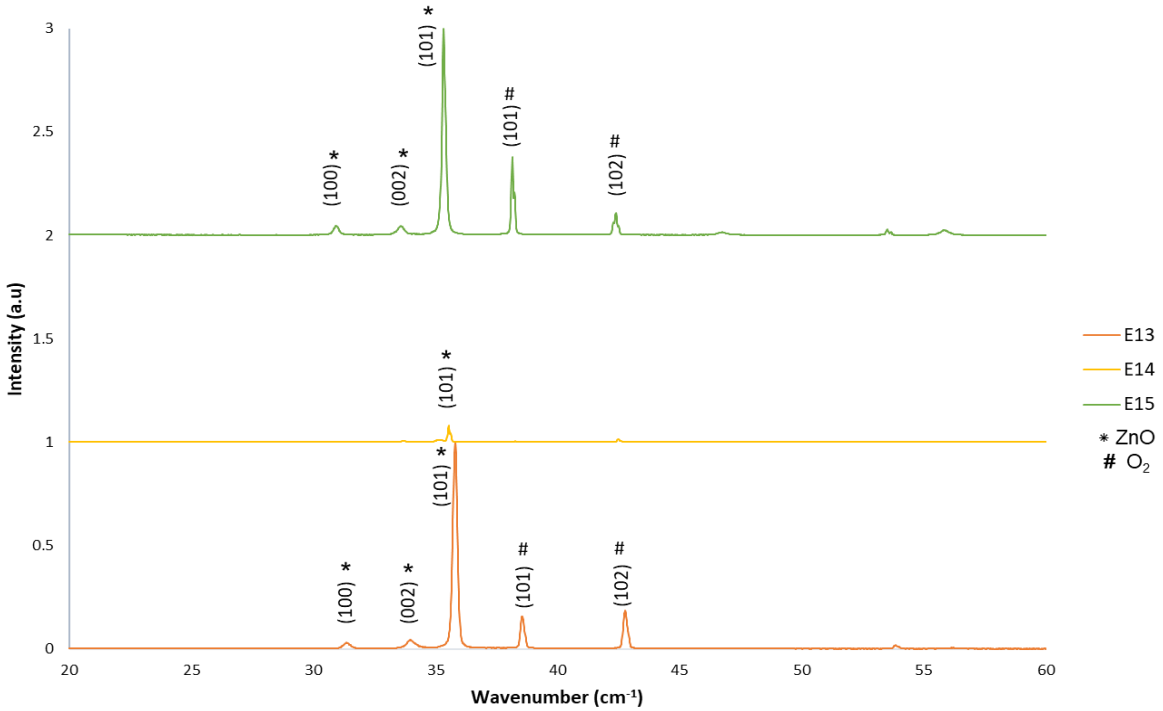

Fig. 6. XRD spectra for ZnO with different oxygen gas flow rate

Table 2 shows the average value of crystallite size was 30.95 nm, 61.16 nm and 27.90 nm corresponding to 5%, 10% and 25% of O_2 gas flow rate during ZnO growth. It could be seen that the value of *D* shows an increment as the O_2 gas flow rate increased from 5% to 10% but inclined when the O_2 gas flow rate was further rise to 25%. This is due to an increase in particle agglomeration on the surface of synthesized ZnO for sample E14. The agglomeration of nanoparticles can be observed in FESEM morphology as seen in Figure 3.

Table 2
Measurement and structural calculation of ZnO

Sample	Oxygen gas (%)	hkl plane	Lattice spacing, d	2θ(°)	a (Å)	c (Å)	Crystallite size, D (nm)
E13	5	(101)	2.5030	35.8156	3.2862	5.2598	30.9543
E14	10	(101)	2.5239	35.5403	3.3270	5.2322	61.1580
E15	25	(101)	2.5368	35.3543	3.3468	5.2443	27.9008

Furthermore, it can be observed the position of the diffraction peak was shifted toward the lower angle as the O_2 gas flow rate increased from 5% to 25%. Based on the report from Koutu *et al.,* [34], the E14 sample has a lower diffraction peak intensity than the E15 and E13 samples, which represent crystal plane rearrangement during the growth process. The changes were suggested to be caused by the generation of residual stress as the O_2 flow rate was increased. Tsao *et al.,* [35] also reported that tensile stress was produced along the growth direction as ZnO nanostructures grown at much lower temperatures (400°C) on Si substrates. Consequently, the presence of residual stress indicates the existence of strain in the crystal lattice. The occurrence might be due to a mismatch between the ZnO crystal lattice and the substrate interface during the growth process.

3.4 RAMAN Spectra

Raman data was used to determine the structural defects, crystal perfection and presence of multiple bonding vibrations [16,36]. Figure 7 shows a Raman spectrum for ZnO nanostructures at room temperature measured using 532 nm He-Cd as a laser source. It was reported that synthesized ZnO with wurtzite type belongs to the C^4P63mc space group and eight sets of optical phonon modes near the centre in the Brillouin zone which can be categorized as:

$$\Gamma_{opt} = A_1 + 2B_1 + E_1 + 2E_2$$

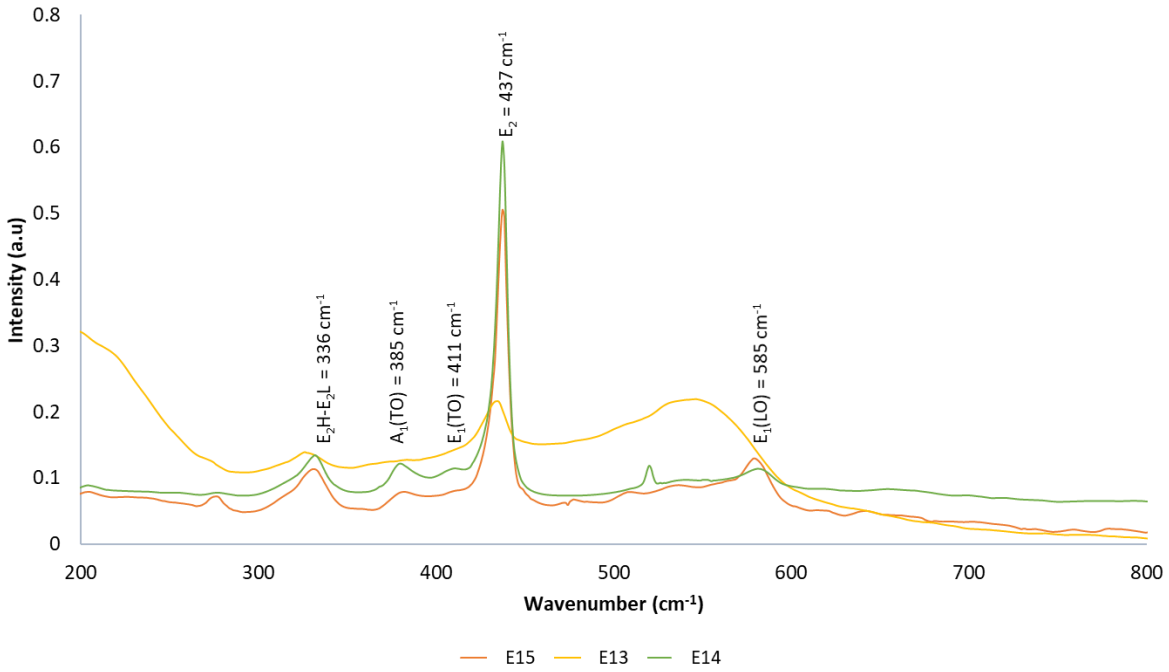

Fig. 7. Raman spectra for synthesized ZnO

All the eight sets of phonons are E_2 modes (Raman active), B_1 (Raman silent), and A_1 + E_1 (infrared active). Raman spectra are highly sensitive to structural defects and crystal quality where the disorder of grown ZnO nanostructures has been evaluated by the nature of detected phonon modes.

From Figure 7, it can be observed a strong and sharp E_2 mode at 439 cm^{-1} and 437 cm^{-1} corresponding to E14 (10% O_2) and E15 (25% O_2) samples confirms that the synthesized ZnO in wurtzite hexagonal phase with high crystallinity.

Meanwhile, the E13 (5% O_2) sample has a low peak of E_2 mode at 433 cm^{-1}. This could be caused by compressive and tensile stress from the vibrations of O_2 atoms in the crystal lattice of ZnO nanostructures [36]. It was supported by a research study from Yoshikawa *et al.,* [37] who found that the decrease in intensity peak of E_2 mode leads to a decrease in crystallite size and causes the peak to broaden. Furthermore, a slightly blue shift towards lower frequency is observed in the E13 sample which is attributed to the effect of internal strain that changes the directions of ZnO growth, and this result corresponds with XRD data. The chemical bonds increased as the atoms of the crystal were pulled out relative to their normal position, resulting in the generation of tensile strain within the ZnO crystal structure [38].

In addition, three observed weak peaks at 336 cm^{-1}, 385 cm^{-1} and 411 cm^{-1} correspond to E_2H-E_2L, A_1(TO) and E_1(TO) modes, respectively. These peaks are attributed to the multiphoton scattering process during the ZnO growth [34,39]. While, E_1L mode was detected at 582 cm^{-1}, 549 cm^{-1} and 585

cm^{-1} for E15, E13 and E14 samples, correspondingly. It shows that the existence of E_1(LO) mode has been related to the generation of some defects from oxygen vacancies, Zn interstitials or free carriers [36,40]. The presence of the high-intensity E_2 mode and weak-intensity E_1L mode in Raman scattering shows that the synthesized ZnO has good crystal quality and possesses a wurtzite hexagonal shape.

3.5 Growth Mechanism

The growth mechanism involved in this study is a combination of self–catalyzed vapor-liquid-solid (VLS) and vapor-solid (VS) mechanisms. It was believed that self-catalyzed VLS was responsible for the nucleation and VS mechanism contributed to further longitudinal growth of nanostructures [41,42]. At first, the Zn powder begins to evaporate at a low melting temperature of 419 ℃ and turns to vapor form. These vapors were subsequently condensed on the surface of the Si wafer as Zn suboxides (ZnO_x where $x < 1$) molten liquid which is an ideal catalyst for ZnO growth and this called as self-catalyzed vapor-liquid-solid (VLS) mechanism. Carrying gases and metal catalysts such as gold or platinum is not necessary for the initial growth of ZnO nanostructures. Oxygen already exists at this rate with extremely low quantities that could result from the outside.

When the temperature was further increased to 800℃ and O_2 gas was introduced into the system, initial ZnO nanoclusters served as catalyzing particles and were the preferred sites for the adsorption of Zn and O_2 atoms. The selection of temperature is crucial for ensuring the complete evaporation of zinc, which serves as the source material. This temperature must be high enough to enable the reaction, yet not so high as to induce the decomposition of ZnO or cause an excessively rapid evaporation of Zn, as noted by Rusli *et al.,* [42] and Rajkumar [43]. Further observed in this study has shown temperatures exceeding 1000°C led to a disordered structure in ZnO nanorods and the optimum temperature is around 800°C. Given that hot tube thermal evaporation (HTTE) is a method of physical vapor deposition, several factors must be taken into account when determining the appropriate temperature [18]. These factors include the type of substrate used, the distance between the source and the substrate, the vacuum pressure and the deposition time.

Zn reacts with oxygen under ambient conditions on the Si wafer leading to the growth of ZnO nanorods. The heating process of Zn powder was continued for 1 hour causing the condensation of Zn and O vapors to add more droplets on the tips of co-existing ZnO nanoclusters. Due to further oxidation of Zn and Zn suboxides, the concentration of oxygen in the droplets increases, resulting in the growth of ZnO nanorods [4,44]. The growth of ZnO nanorods will continue to form as long as the ZnO clusters remain in the liquid state and the reactants (Zn and O) are available. This concluded that ZnO nanostructures were grown in the catalyst-free growth and both self-catalyzed VLS and VS growth were interesting to explore with respect to the cost-effectiveness [26,45].

4. Conclusions

In conclusion, high-quality ZnO nanostructures were successfully grown by hot tube thermal evaporation method under vacuum conditions. The percentage of O_2 and Ar gas flow rate was varied at 5%:95%, 10%:90% and 25%:75% with a growth temperature of 800℃. Altering the percentage ratio of gas flow rate affects the structural and optical properties of synthesized ZnO nanostructures. The growth mechanism has been described by a combination of self-catalyzed VLS and VS mechanisms. FESEM shows a variety of grown nanostructures produced with self-catalyzed growth mechanisms containing nanoparticles, nanoclusters and nanorods. XRD analysis reveals that the ZnO nanostructures exhibited a single crystalline in the wurtzite hexagonal phase and preferentially grew along the c-axis direction. EDS supports the XRD result by showing the pure composition of the

synthesized ZnO as a major percentage occupied by Zinc and O_2 elements. Raman scattering of the obtained ZnO nanostructures show a good crystal quality with a wurtzite hexagonal phase and very less structural defects exist. Among the synthesized ZnO, sample E15 was selected to have an ideal characteristic as it shows high crystallinity with fewer defects resulting from structural and optical properties characterization. Thus, this high quality of ZnO nanostructures may provide opportunities for various practical applications. For future research, it would be beneficial for scientists to investigate the integration of these nanostructures into actual devices. Additionally, experimenting with doping these structures with various materials could further improve their performance, durability, and efficiency under real-world conditions.

Acknowledgment
This research was financially funded by Universiti Sains Islam Malaysia (USIM) under the Research and Innovation Management Centre (RIMC) (PPPI/FST/0121/USIM/15521) grant and all facilities were utilized under the authority of the Faculty of Science and Technology at USIM.

References

[1] Islam, Muhammad R., Mukhlasur Rahman, S. F. U. Farhad, and Jiban Podder. "Structural, optical and photocatalysis properties of sol-gel deposited Al-doped ZnO thin films." *Surfaces and Interfaces* 16 (2019): 120-126. https://doi.org/10.1016/j.surfin.2019.05.007

[2] Kim, Heeran, A. Pique, J. S. Horwitz, H. Murata, Z. H. Kafafi, C. M. Gilmore, and D. B. Chrisey. "Effect of aluminum doping on zinc oxide thin films grown by pulsed laser deposition for organic light-emitting devices." *Thin Solid Films* 377 (2000): 798-802. https://doi.org/10.1016/S0040-6090(00)01290-6

[3] Lide, David R. *CRC handbook of chemistry and physics: a ready-reference book of chemical and physical data*. Boca CRC Press, 1991.

[4] Sakrani, Samsudi, Peshawa Omer Amin, and Syahida Suhaimi. "Zinc Oxide Nanowires Synthesized using a Hot Tube Thermal Evaporation under Intermediate Heating Period." *Malaysian Journal of Fundamental and Applied Sciences* 9, no. 4 (2013): 201-205. https://doi.org/10.11113/mjfas.v9n4.109

[5] Deam, Ahmed Raad, and Shawki Khalaf Muhammad. "Efffect of Copper Doping on the Structural and Optical Properties of ZnO Thin Films Prepared by Thermal Evaporation Method." *Journal of Applied Physical Science International* 7, no. 1 (2016): 35-41.

[6] Taunk, P. B., R. Das, D. P. Bisen, and Raunak Kumar Tamrakar. "Structural characterization and photoluminescence properties of zinc oxide nano particles synthesized by chemical route method." *Journal of Radiation Research and Applied Sciences* 8, no. 3 (2015): 433-438. https://doi.org/10.1016/j.jrras.2015.03.006

[7] Khatibani, A. Bagheri. "Investigation of gas sensing property of zinc oxide thin films deposited by Sol-Gel method: effects of molarity and annealing temperature." *Indian Journal of Physics* 95, no. 2 (2021): 243-252. https://doi.org/10.1007/s12648-020-01689-4

[8] Singh, Jai, and Amit Srivastava. "Morphological evolution and its correlation with optical and field emission properties in pulsed laser deposited ZnO nanostructures." *Materials Science in Semiconductor Processing* 138 (2022): 106282. https://doi.org/10.1016/j.mssp.2021.106282

[9] Khudiar, Ausama I., and Attared M. Ofui. "Effect of pulsed laser deposition on the physical properties of ZnO nanocrystalline gas sensors." *Optical Materials* 115 (2021): 111010. https://doi.org/10.1016/j.optmat.2021.111010

[10] Jayaraman, Vinoth Kumar, Yasuhiro Matsumoto Kuwabara, and Arturo Maldonado Álvarez. "Importance of substrate rotation speed on the growth of homogeneous ZnO thin films by reactive sputtering." *Materials Letters* 169 (2016): 1-4. https://doi.org/10.1016/j.matlet.2016.01.088

[11] Aljameel, A. I., and Mahros Darsin. "Single Crystalline Zinc Oxide Nanorods Grown by RF Sputtering Technique Onto P-Si Substrate for Sensing Applications." *Material Science Research India* 19 (2022): 36-43. https://doi.org/10.13005/msri/190104

[12] Alkahlout, Amal, Naji Al Dahoudi, Ingrid Grobelsek, and Mohammad Jilavi. "Synthesis and characterization of aluminum doped zinc oxide nanostructures via hydrothermal route." *Journal of Materials* 2014 (2014): 235638. https://doi.org/10.1155/2014/235638

[13] Mohan, Sonima, Mini Vellakkat, Arun Aravind, and U. Reka. "Hydrothermal synthesis and characterization of Zinc Oxide nanoparticles of various shapes under different reaction conditions." *Nano Express* 1, no. 3 (2020): 030028. https://doi.org/10.1088/2632-959X/abc813

[14] Pradhan, Prashant, Juan Carlos Alonso, and Monserrat Bizarro. "Photocatalytic performance of ZnO: Al films under different light sources." *International Journal of Photoenergy* (2012). https://doi.org/10.1155/2012/780462
[15] Amroun, M. N., K. Salim, and A. H. Kacha. "Molarities effect on structural optical and electrical properties of nanostructured zinc oxide deposited by spray pyrolysis technique." *International Journal of Thin Film Science and Technology* 10, no. 1 (2021): 67-73. https://doi.org/10.18576/ijtfst/100110
[16] Somvanshi, Divya, and S. Jit. "Synthesis and optical properties of zinc oxide nanoparticles grown on Sn-coated silicon substrate by thermal evaporation method." In *International Conference on Communication and Electronics System Design*, vol. 8760, pp. 91-96. SPIE, 2013. https://doi.org/10.1117/12.2010345
[17] Tsai, Chin-Yi, Jyong-Di Lai, Shih-Wei Feng, Chien-Jung Huang, Chien-Hsun Chen, Fann-Wei Yang, Hsiang-Chen Wang, and Li-Wei Tu. "Growth and characterization of textured well-faceted ZnO on planar Si (100), planar Si (111), and textured Si (100) substrates for solar cell applications." *Beilstein Journal of Nanotechnology* 8, no. 1 (2017): 1939-1945. https://doi.org/10.3762/bjnano.8.194
[18] Raha, Sauvik, and Md Ahmaruzzaman. "ZnO nanostructured materials and their potential applications: progress, challenges and perspectives." *Nanoscale Advances* 4, no. 8 (2022): 1868-1925. https://doi.org/10.1039/D1NA00880C
[19] Abdulgafour, H. I., Naser M. Ahmed, Z. Hassan, F. K. Yam, and A. Sulieman. "Growth evolution and customized attributes of catalyst-free ZnO nanowires: role of varied Ar/O_2 flow rate." *Journal of Materials Science: Materials in Electronics* 31 (2020): 17422-17431. https://doi.org/10.1007/s10854-020-04298-3
[20] Abd Malek, Nur Atiqa, Nor Azwadi Che Sidik, and M'hamed Beriache. "Experimental Study on The Performance of Nano Lubricant in Light Vehicle Engine." *Journal of Advanced Research Design* 83, no. 1 (2021): 1-10.
[21] Vyas, Sumit. "A short review on properties and applications of zinc oxide based thin films and devices: ZnO as a promising material for applications in electronics, optoelectronics, biomedical and sensors." *Johnson Matthey Technology Review* 64, no. 2 (2020): 202-218. https://doi.org/10.1595/205651320X15694993568524
[22] Huang, Chien-Wei, Ru-Yuan Yang, Cheng-Tang Pan, and Min-Hang Weng. "Effect of O_2/Ar Gas Flow Ratios on Properties of Cathodic Vacuum Arc Deposited ZnO Thin Films on Polyethylene Terephthalate Substrate." *Journal of Nanomaterials* 2016 (2016). https://doi.org/10.1155/2016/6479812
[23] Rasheed, H. S., N. M. Ahmed, M. Z. Matjafri, and E. A. Kabaa. "Ar gas flow rate influncement on the structure properties and electrical behavior of new sensing membrane ZnO/Cu/ZnO (ZCZ) extended gate field effect transistor (EG-FET)." *Digest Journal of Nanomaterials & Biostructures (DJNB)* 12, no. 4 (2017).
[24] Camacho-Berrios, Adrian A., Victor M. Pantojas, and Wilfredo Otano. "Reactive sputtered ZnO thin films: Influence of the O_2/Ar flow ratio on the oxygen vacancies and paramagnetic active sites." *Thin Solid Films* 692 (2019): 137641. https://doi.org/10.1016/j.tsf.2019.137641
[25] Hamid, Najiha, Syahida Suhaimi, Muhammad Zamir Othman, and Wan Zakiah Wan Ismail. "A Review on thermal evaporation method to synthesis zinc oxide as photocatalytic material." *Nano Hybrids and Composites* 31 (2021): 55-63. https://doi.org/10.4028/www.scientific.net/NHC.31.55
[26] Choi, Seok Cheol, Do Kyung Lee, and Sang Ho Sohn. "Effects of experimental configuration on the morphology of two-dimensional ZnO nanostructures synthesized by thermal chemical-vapor deposition." *Crystals* 10, no. 6 (2020): 517. https://doi.org/10.3390/cryst10060517
[27] Rusli, Nurul Izni, Masahiro Tanikawa, Mohamad Rusop Mahmood, Kanji Yasui, and Abdul Manaf Hashim. "Growth of high-density zinc oxide nanorods on porous silicon by thermal evaporation." *Materials* 5, no. 12 (2012): 2817-2832. https://doi.org/10.3390/ma5122817
[28] Hasim, Siti Nuurul Fatimah, Muhammad Azmi Abdul Hamid, Roslinda Shamsudin, and Azman Jalar. "Synthesis and characterization of ZnO thin films by thermal evaporation." *Journal of Physics and Chemistry of Solids* 70, no. 12 (2009): 1501-1504. https://doi.org/10.1016/j.jpcs.2009.09.013
[29] Sekar, A., S. H. Kim, A. Umar, and Y. B. Hahn. "Catalyst-free synthesis of ZnO nanowires on Si by oxidation of Zn powders." *Journal of Crystal Growth* 277, no. 1-4 (2005): 471-478. https://doi.org/10.1016/j.jcrysgro.2005.02.006
[30] Hassan, Muhammad, L. Jiaji, P. Lee, and Rajdeep Singh Rawat. "Catalyst free growth of ZnO thin film nanostructures on Si substrate by thermal evaporation." *Applied Physics A* 127, no. 7 (2021): 553. https://doi.org/10.1007/s00339-021-04650-2
[31] Godiwal, Rahul, Amit Kumar Gangwar, Ajay Kumar Verma, Pargam Vashishtha, Ashwani Kumar, Vipin Chawla, Govind Gupta, and Preetam Singh. "Synthesis and growth mechanism of ZnO nanocandles using thermal evaporation and their efficient CO sensing performance." *Micro and Nanostructures* 184 (2023): 207692. https://doi.org/10.1016/j.micrna.2023.207692
[32] Das, Sachindra Nath, Subhasish Patra, Jyoti Prakash Kar, Min-Jung Lee, Sung Hwan Hwang, Tae Il Lee, and Jae-Min Myoung. "Growth and characterization of Mg-doped GaN nanowire synthesized by the thermal evaporation method." *Materials Letters* 106 (2013): 352-355. https://doi.org/10.1016/j.matlet.2013.05.062

[33] Mugwang'a, F. K., P. K. Karimi, W. K. Njoroge, and O. Omayio. "Characterization of aluminum doped zinc oxide (Azo) thin films prepared by reactive thermal evaporation for solar cell applications." *Journal of Fundamentals of Renewable Energy and Applications* 5, no. 4 (2015): 1000170-1000175.
[34] Koutu, Vaibhav, Lokesh Shastri, and M. M. Malik. "Effect of NaOH concentration on optical properties of zinc oxide nanoparticles." *Materials Science-Poland* 34, no. 4 (2016): 819-827. https://doi.org/10.1515/msp-2016-0119
[35] Tsao, F. C., J. Y. Chen, Cheng-Huang Kuo, Gou-Chung Chi, Ching-Jen Pan, P. J. Huang, Chun-Ju Tun et al. "Residual strain in ZnO nanowires grown by catalyst-free chemical vapor deposition on GaN/sapphire (0001)." *Applied Physics Letters* 92, no. 20 (2008). https://doi.org/10.1063/1.2936090
[36] Abdulgafour, H. I., Z. Hassan, N. Al-Hardan, and F. K. Yam. "Growth of zinc oxide nanoflowers by thermal evaporation method." *Physica B: Condensed Matter* 405, no. 11 (2010): 2570-2572. https://doi.org/10.1016/j.physb.2010.03.033
[37] Yoshikawa, M., K. Inoue, T. Nakagawa, H. Ishida, N. Hasuike, and H. Harima. "Characterization of ZnO nanoparticles by resonant Raman scattering and cathodoluminescence spectroscopies." *Applied Physics Letters* 92, no. 11 (2008): 113115. https://doi.org/10.1063/1.2901159
[38] Tuschel, David. "Stress, strain, and Raman spectroscopy." *Spectroscopy* 34, no. 9 (2019): 10-21.
[39] Abdulgafour, H. I., Naser M. Ahmed, Z. Hassan, F. K. Yam, and A. Sulieman. "Growth evolution and customized attributes of catalyst-free ZnO nanowires: role of varied Ar/O_2 flow rate." *Journal of Materials Science: Materials in Electronics* 31 (2020): 17422-17431. https://doi.org/10.1007/s10854-020-04298-3
[40] Decremps, Fredéric, Julio Pellicer-Porres, A. Marco Saitta, Jean-Claude Chervin, and Alain Polian. "High-pressure Raman spectroscopy study of wurtzite ZnO." *Physical Review B* 65, no. 9 (2002): 092101. https://doi.org/10.1103/PhysRevB.65.092101
[41] Kar, Soumitra, Bhola Nath Pal, Subhadra Chaudhuri, and Dipankar Chakravorty. "One-dimensional ZnO nanostructure arrays: Synthesis and characterization." *The Journal of Physical Chemistry B* 110, no. 10 (2006): 4605-4611. https://doi.org/10.1021/jp056673r
[42] Rusli, Nurul Izni, Masahiro Tanikawa, Mohamad Rusop Mahmood, Kanji Yasui, and Abdul Manaf Hashim. "Growth of high-density zinc oxide nanorods on porous silicon by thermal evaporation." *Materials* 5, no. 12 (2012): 2817-2832. https://doi.org/10.3390/ma5122817
[43] Rajkumar, C. "Effect of annealing temperature on response time of ZnO photoconductor fabricated using thermal evaporation technique." *Physica Scripta* 97, no. 11 (2022): 115806. https://doi.org/10.1088/1402-4896/ac95db
[44] Suhaimi, Syahida, Samsudi Sakrani, Nadhrah Md Yatim, and Mohd Azman Hashim. "The structural properties of Sn-doped zinc oxide synthesized by hot-tube thermal evaporation." In *AIP Conference Proceedings*, vol. 1972, no. 1. AIP Publishing, 2018. https://doi.org/10.1063/1.5041226
[45] Wu, Chia Cheng, Dong Sing Wuu, Po Rung Lin, Tsai Ning Chen, and Ray Hua Horng. "Three-step growth of well-aligned ZnO nanotube arrays by self-catalyzed metalorganic chemical vapor deposition method." *Crystal Growth & Design* 9, no. 10 (2009): 4555-4561. https://doi.org/10.1021/cg900557n